Title

Characterization of brown adipose tissue thermogenesis in the naked mole-rat *(Heterocephalus glaber),* a poikilothermic mammal

Authors

Yuki Oiwa[1, 2], Kaori Oka[1], Hironobu Yasui[3, 4], Kei Higashikawa[4, 5], Hidemasa Bono[6], Yoshimi Kawamura[1], Shingo Miyawaki[7], Akiyuki Watarai[8,9], Takefumi Kikusui[8], Atsushi Shimizu[10], Hideyuki Okano[11], Yuji Kuge[4, 5], Kazuhiro Kimura[12], Yuko Okamatsu-Ogura[12*] and Kyoko Miura[1, 11, 13, 14*]

[1] Department of Aging and Longevity Research, Kumamoto University, Kumamoto 860-0811, Japan

[2] Division of Immunobiology, Institute for Genetic Medicine, Hokkaido University, Hokkaido 060-0815, Japan

[3] Laboratory of Radiation Biology, Department of Applied Veterinary Sciences, Faculty of Veterinary Medicine, Hokkaido University, Hokkaido 060-0818, Japan

[4] Central Institute of Isotope Science, Hokkaido University, Hokkaido 060-0815, Japan

17 [5] Laboratory of Integrated Molecular Imaging, Department of Biomedical Imaging,

18 Graduate School of Biomedical Science and Engineering, Hokkaido University,

19 Hokkaido 060-0815, Japan

20 [6] Program of Biomedical Science, Graduate School of Integrated Sciences for Life,

21 Hiroshima University, 3-10-23 Kagamiyama, Higashi-Hiroshima, Hiroshima 739-0046,

22 Japan

23 [7] Laboratory of Epigenome Dynamics, Graduate School of Frontier Biosciences, Osaka

24 University, 1-3 Yamadaoka, Suita, Osaka, 565-0871, Japan

25 [8] Companion Animal Research, School of Veterinary Medicine, Azabu University,

26 Sagamihara 252-5201, Japan

27 [9] Laboratory of Behavioral Neuroscience, Institute for Quantitative Biosciences, The

28 University of Tokyo, 113-0032, Tokyo, Japan

29 [10] Division of Biomedical Information Analysis, Iwate Tohoku Medical Megabank

30 Organization, Disaster Reconstruction Center, Iwate Medical University, Shiwa

31 028-3694, Japan

[11] Department of Physiology, Keio University School of Medicine, Tokyo 160-8582, Japan

[12] Laboratory of Biochemistry, Faculty of Veterinary Medicine, Hokkaido University, Hokkaido 060-0818, Japan

[13] Center for Metabolic Regulation of Healthy Aging, Kumamoto University, Kumamoto 860-8556, Japan

[14] Lead Contact

* Correspondence:

miurak@kumamoto-u.ac.jp (K. M.)

y-okamatsu@vetmed.hokudai.ac.jp (Y.O.-O.)

Abstract (within 200 words)

The naked mole-rat (NMR) is a poikilothermic mammal that forms eusocial colonies consisting of one breeding queen, several breeding kings, and subordinates. Despite their poikilothermic feature, NMRs possess brown adipose tissue (BAT), which in homeothermic mammals induces thermogenesis in cold environments. However,

NMR-BAT thermogenic potential is controversial, and its physiological roles are unknown. Here, we show that NMR-BAT has beta-3 adrenergic receptor (ADRB3)-dependent thermogenic potential, which contributes to thermogenesis in the isolated queen in non-cold environments. NMR-BAT expressed several brown adipocyte marker genes and showed noradrenaline-dependent thermogenic activity *in vitro* and *in vivo*. Although our ADRB3 inhibition experiments revealed that NMR-BAT thermogenesis slightly delays the decrease in body temperature in a cold environment, it was insufficient to maintain the body temperatures of the NMRs. In a non-cold environment, NMRs are known to increase their body temperature by a heat-sharing behavior. Interestingly, we found that the body temperatures of NMRs isolated from the colony were also significantly higher than the ambient temperature. We also show that queens, but not subordinates, induce BAT thermogenesis in isolated, non-cold conditions. Our research provides novel insights into the role and mechanism of thermoregulation in this unique poikilothermic mammal.

Introduction

Non-shivering thermogenesis in brown adipose tissue (BAT) helps maintain the body temperatures of homeothermic mammals in cold environments [1]. BAT specifically expresses uncoupling protein 1 (UCP1), which dissipates the energy produced from lipid and glucose metabolism as heat, rather than adenosine triphosphate synthesis, by increasing the proton conductance of the inner mitochondrial membrane. Recently, BAT has also been shown to be involved in thermogenesis in non-cold environments in response to stimuli, such as diet, social defeat, handling, or the presence of an intruder [2–5]. The detailed mechanisms involved in this process have been intensively explored to develop novel treatments for diabetes and other metabolic diseases, because BAT thermogenesis improves lipid and glucose metabolism [6–9]. Interestingly, BAT has also been found in non-homeothermic mammals, which cannot maintain their body temperatures in cold environments [10,11]. However, its function in these animals remains largely obscure.

The naked mole-rat (NMR; *Heterocephalus glaber*; Fig. 1a) is an African poikilothermic mammal that is hairless with thin skin and is known as the longest-living rodent in the world, with extraordinary cancer resistance [12–14]. NMRs live in colonies

80 comprising many individuals (average 70–80 individuals) and form complex
81 underground systems of tunnels, which can reach a total length of 3–5 km per colony,
82 and maintain a warm and relatively constant air temperature [15,16]. These tunnels
83 connect chambers that are used for different activities, including nests, toilets, food
84 storage sites, and garbage spots. Interestingly, poikilothermic NMRs in a colony can
85 temporarily maintain "behaviorally homeothermic" states, regulating their body
86 temperatures by returning to their nest chamber and huddling together to share heat
87 and become warmer, or moving to cooler areas within the tunnel network to decrease
88 their body temperatures [17,18]. In our laboratory, NMRs are housed in acrylic chambers
89 connected by acrylic tunnels that are maintained at 30 ± 0.5°C, which represents a
90 non-cold environment for NMRs (Fig. S1) [19]. NMRs are also known for their unique
91 eusociality – in a colony of up to 300 individuals, only one female (queen) and one to
92 three males (kings) are reproductive, with all other members being sexually immature
93 and working as subordinates [20,21].

94 Daly et al. have previously reported that NMRs have BAT in the interscapular
95 region and in the area around the cervix [10]. However, a previous work examining the

thermogenic potential of NMR-BAT remains controversial. One previous study suggested that NMR-BAT can induce non-shivering thermogenesis based on indirect evidence from the *in vivo* oxygen consumption rate of NMRs after noradrenaline injection [22]. However, to our knowledge, no direct evidence of NMR-BAT thermogenesis has been reported to date. Moreover, Buffenstein et al. have reported that NMRs cannot maintain their body temperatures in cold environments due to their inability to induce persistent non-shivering thermogenesis [19]. NMR-specific mutations in the *UCP1* gene are thought to contribute to this inability [23]. In general, the physiological role of BAT in poikilothermic NMRs is still completely unclear.

In this study, we investigated the molecular and histological characteristics of NMR-BAT, its thermogenic ability, and the NMR-BAT thermogenesis in physiological conditions. We demonstrate that NMRs possess a substantial amount of BAT with thermogenic activity. Although NMR-BAT thermogenesis slightly delays the decrease in body temperature in a cold environment, it was insufficient to maintain the body temperatures of the NMRs. Interestingly, NMR queens, but not subordinates, induce BAT thermogenesis when in an isolated, non-cold situation. Our results reveal that the

NMR-BAT is indeed thermogenic and induces thermogenesis in physiological, cold, and non-cold environments, providing new insights into the process of thermoregulation in this poikilothermic rodent.

Results

Identification and examination of thermogenic BAT in naked mole-rats

We first performed a detailed characterization of NMR-BAT through dissection and a histological analysis. We identified two types of BAT around the cervix of NMRs: subcutaneous light BAT (lBAT), located in the interscapular region and around the cervix, and dark BAT (dBAT), located in deep regions under the cervical muscle (Figs. 1b and S2a). Hematoxylin–eosin (HE) staining and the isolation of adipocytes showed that dBAT mostly consisted of multilocular adipocytes, whereas lBAT was comprised of a mixture of multilocular and unilocular adipocytes (Figs. 1b and S2b). Because thermogenically active adipocytes contain smaller lipid droplets than inactive adipocytes [24], we measured the size of the lipid droplets in the HE-stained images, which showed that dBAT contained significantly smaller lipid droplets than the interscapular BAT of

Crl:CD1 (ICR) mice (Fig. S2c). The average percentage of the total BAT per gram body weight was 1.88% (Fig. S2d).

Quantitative reverse transcription-polymerase chain reaction (qRT-PCR) showed that brown adipocyte marker genes reported in humans [25] and mice [26], such as *UCP1*, Zic family member 1 (*ZIC1*), peroxisome proliferator-activated receptor gamma coactivator 1 alpha (*PGC1α*), and iodothyronine deiodinase 2 (*DIO2*), were highly expressed in dBAT and lBAT (Figs. 1c and S2e). In contrast, for beige adipocyte, an inducible type of thermogenic adipocyte [25, 26], such as T-box transcription factor (*TBX1*) and transcriptional coactivator of the p300/CBP-mediated transcription complex (*CITED1*), were not upregulated in dBAT or lBAT (Figs. 1c and S2e). A gene ontology enrichment analysis further showed that processes related to the generation of precursor metabolites and energy, including the monocarboxylic acid metabolic process, acyl-CoA metabolic process, mitochondrial electron transport, electron transport from ubiquinol to cytochrome c, triglyceride metabolic process, response to fatty acid, glucose 6-phosphate metabolic process, and electron transport from cytochrome c to oxygen, were activated in dBAT, indicating that active metabolism occurs in this tissue

144 (Fig. S2f). Furthermore, the western blotting showed that the UCP1 protein is highly
145 expressed in dBAT and lBAT (Fig. S3).

146 To directly evaluate the thermogenic ability of NMR-BAT, we measured its
147 temperature and the rectum temperature following the administration of noradrenaline by
148 inserting a thermo-probe into the BAT and rectum of anesthetized NMRs. We found that
149 noradrenaline injection caused the BAT temperature to increase by approximately 1.2°C,
150 following which the rectum temperature gradually increased by 0.6°C (Fig. 1d). A
151 positron emission tomography/computed tomography (PET/CT) analysis further showed
152 that 2-deoxy-2-[^{18}F]fluoro-D-glucose ([^{18}F]FDG) was strongly taken up by the BAT of the
153 noradrenaline-injected NMRs, with a clear “neck warmer”-like distribution of [^{18}F]FDG
154 around the cervix, in addition to its presence in the interscapular regions (Fig. 1e and
155 Video S1).

156 To evaluate whether NMR-BAT thermogenesis depends on the adrenergic
157 beta-3 receptor (ADRB3), which plays a critical role in BAT thermogenesis and has a
158 relatively specific expression in the adipose tissues[1], we measured
159 noradrenaline-induced oxygen consumption rate of brown adipocytes isolated from a

mixture of dBAT and lBAT after a noradrenaline treatment in the presence or absence of the ADRB3 inhibitor SR59230A, using adipocytes isolated from a mixture of dBAT and lBAT. We found that the stimulation with noradrenaline caused the rapid increase in oxygen consumption rate of brown adipocytes, but this increase was inhibited by the pre-treatment with SR59230A (Fig. 1f). Together, these findings indicate that poikilothermic NMRs possess ADRB3-dependent thermogenic BAT.

Induction of NMR-BAT thermogenesis that slightly delays the decrease in body temperature in a cold environment

Next, we investigated the roles of NMR-BAT in physiological conditions. Because NMR skin is almost hairless and quite thin (Fig. 1a), BAT thermogenesis can be monitored by measuring the cervix surface temperature with a thermal camera. We found that the cervix surface temperature was correlated with the BAT temperature, as measured by the thermo-probe (Fig. S4). We measured the cervix temperatures of each NMR in the isolated situation because NMRs are known to enter a behaviorally homeothermic state by engaging in a heat-sharing behavior among others in their colony [17,18].

176 To evaluate the thermogenic ability of BAT in a cold environment for NMRs
177 (20°C), we monitored the cervix surface temperature and the abdominal core body
178 temperature of free-moving NMR subordinates using a thermal camera and a
179 temperature telemetry system simultaneously. When NMRs were isolated from the
180 colony and transferred to a room at 20 °C, the body and cervix surface temperatures
181 gradually reduced, indicating NMRs were unable to keep their body temperature in cold
182 environment as previously reported [19]. We found that SR59230A initially accelerated the
183 drops in both temperatures; however, SR59230A did not induce further decrease at
184 equilibrium (Fig. 2a–c). These results suggest that, although BAT thermogenesis
185 contributed to the delay in the decrease in body temperature after cold exposure, the
186 NMRs were unable to maintain their body temperature at 20°C as previously reported [19]
187 (Fig. 2a–c).
188
189 **Induction of BAT thermogenesis in naked mole-rat queens under isolated,**
190 **non-cold conditions**

We found that BAT thermogenesis had a slight but insufficient effect on supporting the body temperature of NMRs in a cold environment (Fig. 2). Therefore, we hypothesized that NMR-BAT may also play a role in non-cold environments. Interestingly, we found that NMRs isolated from their colony did not decrease their body temperatures and also showed higher body temperature than the ambient temperature (Fig. 3a). To test whether the thermogenesis of the isolated subordinates depended on BAT, we injected NMRs with the ADRB3 inhibitor SR59230A and again measured the body temperature of individuals after isolation. However, no significant change was observed in the subordinates (Fig. 3b, c).

Notably, we found that the queens showed a tendency toward higher oxygen consumption rates than other members, suggesting that the BAT of queens may be more thermogenic than in other colony members in this situation (Fig. 3d). Although the body weight and age were higher in queen than in the subordinates [27], we also found that the body weight and age were weakly negatively correlated with the body temperatures of the isolated subordinate NMRs (Fig. S5a, b), suggesting that the higher thermogenic activity of queens was not related to their heavier body weights or older ages. No

207 significant differences in body temperature were found between the sexes (Fig. S5c). To
208 test whether the thermogenesis of the isolated queens depended on BAT, we injected
209 NMRs with the ADRB3 inhibitor SR59230A and again measured the body temperature of
210 individuals after isolation. As a result, we found that the body temperatures of the socially
211 isolated queens significantly decreased following SR59230A injection (Fig. 3e, f). These
212 results indicate that NMR queens, but not subordinates, activate BAT thermogenesis in
213 an isolated, non-cold environment.
214

215 **Discussion**

216 In this study, we provided direct evidence in support of the thermogenic potential of BAT
217 in poikilothermic NMRs, which is ADRB3 dependent. We show that BAT thermogenesis
218 was insufficient to maintain the body temperatures of the NMRs in a cold environment
219 although it can slightly delay the decrease in the body temperatures of NMRs.
220 Furthermore, in a non-cold environment, BAT thermogenesis contributes to maintaining
221 the body temperature of the isolated queen. This research provides *in vitro* and *in vivo*

evidence of NMR-BAT thermogenesis in physiological conditions that have not previously been studied.

A previous study suggested that the NMR *UCP1* gene has a unique sequence that may contribute to the inability of thermogenesis in NMRs [23]; however, our results clearly show that, NMR-BAT does have thermogenic potential (although we did not compare the levels of thermogenic ability of NMR-BAT with those of other species). Whether NMR-BAT has more or less thermogenic potential than the BAT of other species is an important question for future research.

Although our results clearly showed the thermogenic ability of NMR-BAT, NMRs could not maintain their body temperatures in a cold environment (20 °C) as previously described[19]. This result may reflect the fact that NMRs have high heat dissipation because of their thin and hairless skin.

Interestingly, we observed that only queens induce BAT thermogenesis when in an isolated, non-cold situation. Previous reports in mice and rats have indicated that social isolation affects the metabolism and volume of adipose tissues, including BAT [29,30], and that psychological stresses, such as social defeat [3], handling, [4] or the presence

of an intruder, [5] have been shown to induce BAT thermogenesis. Recent studies have revealed that cortisol concentration was also upregulated in NMRs after social isolation [31,32], suggesting that social isolation induces psychological stress in NMRs. Although the differences in stress levels between the queen and other colony members and the neurological systems to transmit the stress to BAT during social isolation in NMRs are still unknown, such differences may contribute to the observed difference in BAT thermogenesis in the isolated situation. Another possibility is that the difference in the BAT thermogenesis between the queen and the other members may result from differences in the thermogenic function or volume of BAT.

However, we were unable to collect and examine BAT from the queen by dissection due to the limited number of queens in our laboratory. Therefore, further experiments are required to investigate the mechanism underlying this queen-specific activation of BAT under isolation in a non-cold environment. Moreover, our observations suggest the possibility that the queen might be more resistant to decreasing body temperature in a cold environment than other members. However, we could not measure the core body temperature of the queen in a cold environment by inserting the

thermo-probe into the abdominal cavity because this would have been too invasive, and the number of reproductive queens was quite limited. However, elucidating this factor will be another important issue for future works.

Moreover, in subordinates, we observed higher body temperatures than the ambient temperatures in a non-cold environment; however, the ADRB3 inhibitor did not decrease the body temperature. Although we cannot deny the possibility that more sensitive measurements can provide different results, our results may suggest that the isolated subordinates increase their body temperatures by BAT-independent mechanisms such as activity-dependent thermogenesis.

A current open question remains whether NMRs staying together in the colony also induce BAT thermogenesis. However, NMRs display the heat-sharing behavior only when inside the colony, and the intraperitoneal injection of SR59230A is not suitable for suppressing BAT thermogenesis for a long time period. Although we tried to irreversibly suppress BAT thermogenesis by cutting the sympathetic nerve projecting into the BAT, we failed because this method was too invasive. Developing methods that suppress BAT thermogenesis for long time periods and allow for a more

sensitive measurement of BAT temperatures will contribute to the further understanding of the function and role of NMR-BAT.

In conclusion, we revealed that the poikilothermic NMR-BAT is thermogenic, inducing thermogenesis in physiological, cold, and non-cold environments. This work provides novel insights into the previously unclear role of BAT in this poikilothermic mammal. Further studies of BAT thermogenesis in the NMR and other non-homeothermic animals should continue to advance our understanding of the unexpected roles of BAT in animal homeostasis.

Materials and Methods

Study organisms

The NMRs used in this study were maintained at Kumamoto University, Kumamoto, Japan, where they were housed in four to 10 acrylic chambers that were connected by acrylic tunnels, at 30 ± 0.5°C and 55% ± 5% humidity with a 12 h light/12 h dark cycle (Fig. S1). The body temperatures of NMRs in the colony were assessed using 1- to 12-year-old NMRs. The effect of social isolation was assessed using 1- to 13-year-old

subordinates, 5- to 13-year-old queens, and 6- to 12-year-old kings. Jcl:ICR mice were purchased from CLEA Japan, Inc., and adipose tissues were collected from 1- to 2-year-old subordinates and 6-week-old mice for cytological and histological analyses.

All experimental procedures were permitted by the Institutional Animal Care and Usage Committees of Kumamoto University (Approval No. A30-043) and Hokkaido University (Approval No. 14-0065).

HE staining and measurement of the lipid droplet size

The NMR and mouse adipose tissues were fixed with 4% paraformaldehyde in phosphate-buffered saline. HE staining was performed by Sapporo General Pathology Laboratory Co., Ltd. (Hokkaido, Japan), and images of the HE-stained samples were acquired with a BZ-X 710 fluorescence microscope (Keyence). The lipid droplet size was measured using a BZ-X image analyzer (Keyence).

mRNA-sequencing analysis

RNA was extracted using Trizol reagent (Life Technologies) in accordance with the manufacturer's protocol. A Qiagen RNeasy column was used for further purification, and genomic DNA was excluded using the TURBO DNA-free™ kit (Invitrogen). RNA quantity and quality were measured by Qubit (Invitrogen) and a 2100 Bioanalyzer using the RNA 6000 Nano Kit (Agilent Technologies). The TruSeq RNA Library Prep Kit v2 (Illumina) was used for library preparation in accordance with the manufacturer's protocol. The acquired library was quantified using the High Sensitivity DNA Kit (Agilent Technologies) and Kapa Library Quantification Kit (Kapa Biosystems) with the Applied Biosystems ViiA7™ Real-Time PCR System (Applied Biosystems) using the manufacturer's protocol. The library was loaded into a flow cell for cluster generation with the TruSeq Rapid SR Cluster Kit (Illumina) and was sequenced using the Illumina Hiseq 2500 System to obtain single-end 100-nucleotide sequences.

The NMR reference genome (HetGla_female_1.0) and annotation files downloaded from Ensembl 92 (https://www.ensembl.org) were used for data analysis. The acquired fastq files were trimmed using Trim Galore ver. 0.4.4. [33], and the transcript

316 abundances (transcripts per million [TPM]) in the trimmed fastq files were calculated
317 using RSEM ver. 1.2.31 with Bowtie 2 [34,35].

318 For the gene ontology enrichment analysis, the calculated TPM of dBAT was
319 compared with that of inguinal white adipose tissue, and the top 200 upregulated genes
320 in dBAT were analyzed by Metascape using gene ontology annotation of the mouse [36].

321

322 **qRT-PCR**

323 Total RNA was extracted using the RNeasy Lipid Tissue Mini Kit (Qiagen), and genomic
324 DNA was eliminated using the TURBO DNA-free Kit (Invitrogen) following the
325 manufacturers' protocols. Reverse transcription reactions were carried out using
326 ReverTra Ace® qPCR RT Master Mix (TOYOBO) with 300 ng of RNA as a template.
327 The resulting cDNA was prepared for qPCR using Thunderbird® qPCR Mix (TOYOBO)
328 in a 384-well plate with the primers listed in Table S1. qPCR was performed on a
329 CFX384 Touch™ Real-Time PCR Detection System (BIO-RAD).

330

331 ***In vivo* measurement of BAT thermogenesis**

NMRs were anesthetized with 0.1 μg/g medetomidine hydrochloride (Dorbene® Vet; Kyoritsu Seiyaku Co.), 4 μg/g midazolam (Dormicum®; Asteras Pharma Inc.), and 5 μg/g butorphanol (Vetorphale; Meiji Seika Pharma Co.). BAT and rectum temperatures were simultaneously measured using a thermo-probe (plastic-coated thermistor, 1 mm diameter). To measure the BAT, the skin above the interscapular region was incised without injury to the vasculature and nerves, and the thermo-probe was inserted under the lBAT. A thermo-probe was also inserted into the rectum at the same time. Once the BAT and rectum temperatures stabilized, 1 mg/kg noradrenaline was injected into the abdominal cavity, and the temperatures of the BAT and rectum were recorded over 30 min. All procedures were performed in a non-cold environment (30 ± 0.5°C), and the NMRs were placed on a hot plate at 32°C (NHP-M30N; NISSIN RIKA) during the experiment.

In vivo measurement of oxygen consumption

The *in vivo* oxygen consumption rate was measured using an O_2/CO_2 metabolism-measuring system (MK-5000RQ6; Muromachi Kikai) and MMS-ML/6

348 software (Muromachi Kikai). The oxygen consumption of a single NMR was measured
349 at 30 ± 0.5°C in a sealed chamber. The NMRs were habituated to the sealed chamber
350 for 2 h prior to testing, and the oxygen consumption rate was recorded for 4 h during the
351 daytime.
352
353 ***In vitro* measurement of adipocyte oxygen consumption**
354 NMR brown adipocytes were isolated from lBAT and dBAT as previously described [37].
355 Briefly, incised NMR adipose tissues were incubated in Krebs–Ringer
356 bicarbonate-HEPES (KRBH) buffer (130 mM Na^+, 4 mM K^+, 0.75 mM Ca^{2+}, 1 mM Mg^{2+},
357 121.5 mM Cl^-, 10 mM HCO_3^-, 1 mM Mg^{2+}, 4 mM HPO_4^{2-}, 30 mM HEPES, and pH 7.4)
358 with 1% fatty acid-free bovine serum albumin (Wako), 6 mM glucose, and 1 mg/mL
359 collagenase (Sigma) at 37°C for 1 h, with shaking at 90 rpm/min. After filtering the
360 suspension through a 200 μM nylon filter, the filtrate was centrifuged at 50 × g for 2 min.
361 The floating adipocytes were then collected and diluted with KRBH buffer containing 4%
362 bovine serum albumin and 2.7 mM glucose and then recentrifuged and washed three

363 times. The acquired adipocytes were incubated at room temperature for 1h before
364 measurement.

365 The oxygen consumption rate was measured using a Clark-style oxygen
366 electrode in a water-jacketed Perspex chamber at 37°C with the StrathKelvin 782
367 2-Channel Oxygen System (StrathKelvin Instruments). Once the stable oxygen
368 consumption rate had been recorded, noradrenaline was injected into the chamber at a
369 final concentration of 1 μM. To examine the effect of the noradrenaline receptor
370 inhibition, SR59230A (10 μM; Sigma) was injected 10 min before injecting
371 noradrenaline.

372

373 **Measurement of the body temperature in a cold environment via a thermal camera**
374 **and telemetry probe**

375 For the measurement of the cervical temperature and abdominal core temperature in a
376 cold environment (20 ºC), we first injected saline or 20 mg/kg SR59230A to the NMR
377 abdominal cavity in a non-cold environment (30 ºC). Then, we moved the NMR in the
378 acrylic cage to a cold environment (20 ºC) and measured changes in the cervical

379 temperature with the thermal camera and the abdominal core temperature by telemetry
380 probe every 5 min for 90 min. Body surface temperatures were monitored using a
381 thermal camera (CPA-E6A; FLIR), and the acquired data were analyzed by FLIR Tools
382 ver. 2.1 (FLIR). The abdominal core body temperature was measured using a telemetric
383 probe (G2 E-mitter; STARR Life Sciences Corp.) and an ER4000 receiver (STARR Life
384 Sciences Corp.). The G2 E-mitter was inserted into the abdominal cavity of
385 anesthetized NMRs, and the animals were left for at least 7 days before being used in
386 the experiment. The acquired data were analyzed by VitalView ver. 4.1 (STARR Life
387 Sciences Corp.).
388
389 **Measurement of the body temperature via a thermal camera in a non-cold**
390 **environment**
391 For the measurement of the cervical temperature of the socially isolated NMRs, we
392 measured the change in the cervical temperature via a thermal camera every 30 min for
393 8 hrs after 30 min social isolation. Individual NMRs were moved from the colony to the
394 acrylic chamber at 30 ± 0.5°C and 55% ± 5% humidity with a 12 h light/12 h dark cycle.

For the measurement of the body temperature in socially isolated NMR to compare against the body weight, age or sex, we measured the change in the cervical temperature via a thermal camera after 30 min of social isolation.

To measure the cervical temperature of the socially isolated NMR with the injection of saline or 20 mg/kg SR59230A to the NMR abdominal cavity, we measured the change in the cervical temperature using the thermal camera every 5 min for 90 min in a non-cold environment (30 ºC) after 30 min of social isolation and the injection of saline or SR59230A.

PET-CT imaging

For PET-CT imaging, NMRs were fasted overnight and kept at 30 ± 0.5°C and 60% humidity. The NMRs were administered 1 mg/kg noradrenaline, following which 11 MBq [^{18}F]FDG was injected into the abdominal cavity. PET-CT images were then acquired 1 h after [^{18}F]FDG administration using the Inveon small-animal multimodality PET/CT system (Siemens Medical Solutions). PET scanning was performed for 10 min followed by CT scan. During this experiment, the NMRs were maintained under isoflurane

411 anesthesia and were kept at 32°C. Acquired PET images were reconstructed using the
412 filtered backprojection algorithm with the ramp filter cut-off at the Nyquist frequency. The
413 image matrix was 256 × 256 × 318, resulting in a voxel size of 0.388 × 0.388 × 0.398
414 mm^3. CT images were reconstructed using a Feldkamp cone-beam algorithm, with a
415 Shepp–Logan filter.
416
417 **Western blotting**
418 Each adipose tissue was dissected, lysed in the buffer (125 mM Tris-HCl, pH 6.8; 4%
419 SDS and 10% sucrose), and boiled for 10 min. After centrifuging, the supernatant was
420 collected. The protein concentration was measured by TaKaRa BCA Protein Assay Kit
421 (Takara Bio) in accordance with the manufacturer's protocol. The 15 μg proteins were
422 subjected to polyacrylamide gel electrophoresis, and then proteins were transferred to
423 the polyvinylidene fluoride membrane. Blocking was performed with 0.5% skim milk for
424 1 h at room temperature. Blotted membranes were incubated with the primary antibody
425 overnight at 4°C and the secondary antibody for 1 h at room temperature. We used
426 anti-UCP-1 antibody (Sigma, U6382; 1:1000) and HRP-conjugated anti-rabbit IgG

427 secondary antibodies (CST, #7074; 1:1000). The membrane was visualized by using
428 Amersham ECL Prime Western Blotting Detection Reagent (GE Healthcare) and
429 ImageQuant LAS 4000 Mini (GE Healthcare).
430 The detected membrane was washed by tris-buffered saline Tween-20 for 10
431 min. Then, the membrane was incubated with Ponceau-S staining solution for 15 min at
432 a room temperature. After discarding the Ponceau-S staining solution, the membrane
433 was incubated with 0.1% acetic acid for 2 min at room temperature. Then, the
434 membrane was dried.
435
436 **Statistical analysis**
437 GraphPad Prism (GraphPad) was used for the statistical analysis. Data were analyzed
438 using one-way analysis of variance followed by Tukey's multiple comparison test with a
439 single pooled variance for multiple comparisons or by Dunnet's multiple comparison test
440 with a single pooled variance. Two groups were compared using an unpaired *t*-test. All
441 values are presented as means ± SD or means ± SEM, as noted.
442

Acknowledgments

We thank Dr. T. Chujo for proofreading the manuscript; Prof. K. Seino, Prof. A. Takaoka, Prof. K. Tomizawa, Prof. Y. Ando, Dr. J. Kohyama, and professors at Institute for Genetic Medicine, Hokkaido University, Faculty of Life Sciences, Kumamoto University, and Institute of Molecular Embryology and Genetics, Kumamoto University for their administrative support and scientific discussion; Y. Sugiura for scientific discussion, Jane Doe of the Liaison Laboratory Research Promotion Center for technical support; I. Koya for the assistance of mRNA-sequencing; Y. Tanabe, Y. Fujimura, and M. Kobe for help with animal maintenance; T. Ohori for assistance in measuring NMR body surface temperatures; and all members of the K. Kimura and K.M. laboratories for technical assistance and scientific discussion. This research was supported in part by grants from the Ministry of Education, Culture, Sports, Science and Technology (MEXT) under grant number 26111006 (Grant-in-Aid for Scientific Research on Innovative Areas ‘Oxygen Biology: a new criterion for integrated understanding of life’), 15H05649 and 18H02365; PRESTO of the Japan Science and Technology Agency under grant number

458 JPMJPR12M2; the Japan Agency of Medical Research and Development (AMED)

459 under grant number JP19gm5010001.

460 K.M. was also supported by The Takeda Science Foundation, The Mitsubishi

461 Foundation, The Naito Foundation, The Nagase Science and Technology Foundation,

462 The Kurata Memorial Hitachi Science and Technology Foundation, The Nakajima

463 Foundation, and The Suzuken Memorial Foundation.

464

465 **Contributions**

466 Y.O. conducted most of the experiments; K.O., H.Y., K.H., and Y.K. conducted the

467 PET-CT experiments; H.B., Y.K., S.M., A.S., and H.O. supported the

468 mRNA-sequencing experiments and analysis; W.A., T.K., Y.S., and M.S. supported the

469 characterization of brown adipose tissue; Y.O.-O., and K.K supported the BAT oxygen

470 consumption rate measurements; Y.O., Y.O.-O., and K.M. designed the study; Y.O.,

471 Y.O.-O., and K.M. wrote the manuscript; Y.O.-O. and K.M. supervised the research.

472

473 **Accession code**

RNA-seq data have been deposited in the DNA Data Bank of Japan database under accession code: DRA007737. Gene expression abundance data have also been deposited in the Genomic Expression Archive under accession code: E-GEAD-294.

Competing financial interest statement

The authors declare that there are no competing financial interests.

Reference

1. Cannon, B. & Nedergaard, J. Brown adipose tissue: function and physiological significance. *Physiol. Rev.* **84**, 277–359 (2004).

2. Rothwell, N. J. A role for brown adipose tissue in diet-induced thermogenesis. *Obes. Res.* **5**, 650–6 (1997).

3. Kataoka, N., Hioki, H., Kaneko, T. & Nakamura, K. Psychological stress activates a dorsomedial hypothalamus-medullary raphe circuit driving brown adipose tissue thermogenesis and hyperthermia. *Cell Metab.* **20**, 346–58 (2014).

4. Zhang, W. *et al.* Orexin neurons are indispensable for stress-induced

490 thermogenesis in mice. *J. Physiol.* **588**, 4117–29 (2010).

491 5. Mohammed, M., Ootsuka, Y. & Blessing, W. Brown adipose tissue

492 thermogenesis contributes to emotional hyperthermia in a resident rat suddenly

493 confronted with an intruder rat. *Am. J. Physiol. Integr. Comp. Physiol.* **306**, R394-400

494 (2014).

495 6. Rosen, E. D. & Spiegelman, B. M. Adipocytes as regulators of energy balance

496 and glucose homeostasis. *Nature* **444**, 847–53 (2006).

497 7. Bartelt, A. *et al.* Brown adipose tissue activity controls triglyceride clearance.

498 *Nat. Med.* **17**, 200–5 (2011).

499 8. Thomou, T. *et al.* Adipose-derived circulating miRNAs regulate gene

500 expression in other tissues. *Nature* **542**, 450–455 (2017).

501 9. Kajimura, S., Spiegelman, B. M. & Seale, P. Brown and beige fat:

502 Physiological roles beyond heat generation. *Cell Metabolism* (2015).

503 doi:10.1016/j.cmet.2015.09.007

504 10. Daly, T. J., Williams, L. A. & Buffenstein, R. Catecholaminergic innervation of

505 interscapular brown adipose tissue in the naked mole-rat (Heterocephalus glaber). *J*

506 *Anat* **190 (Pt 3)**, 321–326 (1997).

507 11. Oelkrug, R. *et al.* Brown fat in a protoendothermic mammal fuels eutherian

508 evolution. *Nat. Commun.* **4**, 2140 (2013).

509 12. Jarvis, J. U. M. & Bennett, N. C. Ecology and Behavior of the Family

510 Bathyergidae. in *The biology of the Naked Mole-Rat* 66–96 (1991).

511 13. Buffenstein, R. Negligible senescence in the longest living rodent, the naked

512 mole-rat: Insights from a successfully aging species. *J. Comp. Physiol. B Biochem. Syst.*

513 *Environ. Physiol.* **178**, 439–45 (2008).

514 14. Miyawaki, S. *et al.* Tumour resistance in induced pluripotent stem cells derived

515 from naked mole-rats. *Nat. Commun.* (2016). doi:10.1038/ncomms11471

516 15. Bennett, N. C., Jarvis, J. U. M. & Davies, K. C. Daily and seasonal

517 temperatures in the burrows of African rodent moles. *South African J. Zool.* **23**, 189–195

518 (1988).

519 16. Holtze, S. *et al.* The microenvironment of naked mole-rat burrows in East

520 Africa. *Afr. J. Ecol.* **56**, 279–289 (2018).

521 17. Withers, P. C. & Jarvis, J. U. M. The effect of huddling on thermoregulation and

522 oxygen consumption for the naked mole-rat. *Comp. Biochem. Physiol. -- Part A Physiol.*

523 **66**, 215–219 (1980).

524 18. Yahav, S. & Buffenstein, R. Huddling Behavior Facilitates Homeothermy in the

525 Naked Mole Rat Heterocephalus-Glaber. *Physiol. Zool.* **64**, 871–884 (1991).

526 19. Buffenstein, R. & Yahav, S. Is the naked mole-rat Hererocephalus glaber an

527 endothermic yet poikilothermic mammal? *J. Therm. Biol.* **16**, 227–232 (1991).

528 20. Jarvis, J. Eusociality in a mammal: cooperative breeding in naked mole-rat

529 colonies. *Science (80-.).* **212**, 571–3 (1981).

530 21. Watarai, A. *et al.* Responses to pup vocalizations in subordinate naked

531 mole-rats are induced by estradiol ingested through coprophagy of queen's feces. *Proc.*

532 *Natl. Acad. Sci.* **115**, 9264–9269 (2018).

533 22. Hislop, M. S. & Buffenstein, R. Noradrenaline induces nonshivering

534 thermogenesis in both the naked mole-rat (Heterocephalus glaber) and the Damara

535 mole-rat (Cryptomys damarensis) despite very different modes of thermoregulation. *J.*

536 *Therm. Biol.* **19**, 25–32 (1994).

537 23. Kim, E. B. *et al.* Genome sequencing reveals insights into physiology and

longevity of the naked mole rat. *Nature* **479**, 223–227 (2011).

24. Cinti, S. The role of brown adipose tissue in human obesity. *Nutr. Metab. Cardiovasc. Dis.* **16**, 569–74 (2006).

25. Jespersen, N. Z. *et al.* A classical brown adipose tissue mrna signature partly overlaps with brite in the supraclavicular region of adult humans. *Cell Metab.* **17**, 798–805 (2013).

26. de Jong, J. M. A., Larsson, O., Cannon, B. & Nedergaard, J. A stringent validation of mouse adipose tissue identity markers. *Am. J. Physiol. - Endocrinol. Metab.* **308**, E1085-105 (2015).

27. Clarke, F. M. & Faulkes, C. G. Dominance and queen succession in captive colonies of the eusocial naked mole-rat, Heterocephalus glaber. Proc. R. Soc. Lond. B 264, 993–1000 (1997).

28. Chouchani, E. T. *et al.* Mitochondrial ROS regulate thermogenic energy expenditure and sulfenylation of UCP1. *Nature* (2016). doi:10.1038/nature17399

29. Nonogaki, K., Nozue, K. & Oka, Y. Social isolation affects the development of obesity and type 2 diabetes in mice. *Endocrinology* **148**, 4658–4666 (2007).

554 30. Volden, P. A. *et al.* Chronic social isolation is associated with metabolic gene
555 expression changes specific to mammary adipose tissue. *Cancer Prev. Res.* **6**, 634–45
556 (2013).
557 31. Makori, A. O., Nyongesa, A. W., Odongo, H. & Masai, R. J. Assessment of
558 Stress on Serum Estradiol and Cortisol Levels in Female Subordinate Naked Mole Rats
559 Following Isolation from Natal Colony. *J. Biosci. Med.* (2020).
560 doi:10.4236/jbm.2020.83002
561 32. Edwards, P. D. *et al.* The Stress of Being Alone: Removal From the Colony,
562 but Not Social Subordination, Increases Fecal Cortisol Metabolite Levels in Eusocial
563 Naked Mole-Rats. *Horm. Behav.* **121**, (2020).
564 33. Krueger, F. Trim Galore. *Babraham Bioinformatics* (2016).
565 http://www.bioinformatics.babraham.ac.uk/projects/trim galore/
566 34. Li, B. & Dewey, C. N. RSEM: Accurate transcript quantification from RNA-Seq
567 data with or without a reference genome. *BMC Bioinformatics* **12**, 323 (2011).
568 35. Langmead, B. & Salzberg, S. L. Fast gapped-read alignment with Bowtie 2.
569 *Nat. Methods* **9**, 357–359 (2012).

570 36. Zhou, Y. et al. Metascape provides a biologist-oriented resource for the

571 analysis of systems-level datasets. Nat. Commun 10, 1523 (2019).

572 37. Okamatsu-Ogura Y, Fukano K, Tsubota A, Uozumi A, Terao A, Kimura K,

573 Saito M. (2013) Thermogenic ability of uncoupling protein 1 in beige adipocytes in mice.

574 PLoS One, 8: e84229.

575

576

577

578 **Figure 1. Poikilothermic naked mole-rats (NMRs; *Heterocephalus glaber*) possess**

579 **thermogenic brown adipose tissue (BAT)**

580 **(a)** Photograph of an adult NMR. **(b)** Anatomical (top), hematoxylin–eosin (HE)-stained

581 (middle) and cell (bottom) images of light BAT (lBAT) and dark BAT (dBAT). Scale bar =

582 100 μm for HE-stained images, 25 μm for insets, 200 μm for cell images. **(c)** Relative

583 mRNA expression levels of brown (*UCP1*, *ZIC1*, *PGC1α* and *DIO2*) and beige (*TBX1*

584 and *CITED1*) adipocyte marker genes reported in mouse and human in NMR adipose

585 tissues. Expression levels were quantified by quantitative reverse

586 transcription-polymerase chain reaction (qRT-PCR), normalized to beta-actin (*ACTB*),

587 and compared with lBAT (n = 3 animals). vlBAT, ventral light BAT; ingWAT, inguinal

588 white adipose tissue (WAT); rpWAT, retroperitoneal WAT; gWAT, gonadal WAT. **(d)**

589 BAT and rectum temperatures of anesthetized NMRs before and after the *i.p.* injection of

590 1 mg/kg noradrenaline (arrow) at 30°C (n = 3 animals). **(e)** Positron emission

591 tomography/computed tomography (PET-CT) imaging of NMR-BAT after the injection of

592 1 mg/kg noradrenaline and 11 MBq 2-deoxy-2-[^{18}F]fluoro-D-glucose ([^{18}F]FDG) at 32°C.

593 **(f)** *In vitro* oxygen consumption rates of isolated adipocytes after the injection of 1 μM

noradrenaline (arrow) with or without pre-incubation with 10 μM SR59230A (n = 3 animals per treatment), * $p < 0.05$ significantly different from SR59230A treated cells (paired t-test). All data are presented as means ± SEM with the exception of **(d)**, which are means ± SD.

Figure 2. Brown adipose tissue (BAT) thermogenesis in naked mole-rat (NMR; *Heterocephalus glaber*) subordinates after cold exposure

(a) Thermal images of the declining body surface temperatures of NMRs during cold exposure (20°C) following the injection of saline or 20 mg/kg SR59230A (n = 4 animals per treatment). **(b)** Maximum cervix surface temperatures monitored by a thermal camera (n = 4 animals) and **(c)** abdominal core body temperatures recorded by a telemetry probe inserted into the abdominal cavity (n = 3 animals) of NMRs during cold exposure (20°C) following the injection of saline or 20 mg/kg SR59230A * $p < 0.05$ significantly different from SR59230A treated sample (paired t-test).

Figure 3. Isolated naked mole-rat (NMR; *Heterocephalus glaber*) queen exhibits BAT thermogenesis

(a) Maximum cervix surface temperatures of NMRs staying together in the colony (colony) or isolated from the colony (isolation). In the colony data, each point represents the average temperatures of individual NMRs measured at six times in the colony (three times in the nest and three times outside the nest). In the isolation data, each point represents the average temperatures of individual NMRs recorded every 30 min over 8 h. n = 5 animals for the queen and king, n = 7 animals for the subordinate. Av RT., the average room temperature, **(b)** Representative images and **(c)** time course of changes in the maximum cervix surface temperatures of socially isolated subordinates following the *i.p.* injection of saline or 20 mg/kg SR59230A (n = 3 animals). Measurement began after the isolation-induced increase in cervix surface temperature became stable [* $p < 0.05$ significantly different from SR59230A treated animals (paired t-test)]. Data are presented as means ± SEM. **(d)** Average oxygen consumption rates of the queen and subordinates in a socially isolated state measured in a metabolic cage in a non-cold environment (n = 5 queens, 7 subordinates, and 5 kings). Data collected over 4 h in the daytime after a 2-h

632 habituation period. Data are presented as means ± SEM and were analyzed using

633 one-way analysis of variance followed by Tukey's multiple comparison test with a single

634 pooled variance for multiple comparisons (* $p < 0.05$ significantly different from each

635 groups), **(e)** representative images, and **(f)** time course of changes in the maximum

636 cervix surface temperatures of socially isolated queens, following the *i.p.* injection of

637 saline or 20 mg/kg SR59230A ($n = 5$ animals); * $p < 0.05$ significantly different from

638 SR59230A treated animals (paired *t*-test). Data are presented as means ± SEM.

639

640 **Figure S1. Images of acrylic chambers connected by acrylic tunnels used to**

641 **house the naked mole-rats (NMRs; *Heterocephalus glaber*) in the laboratory**

642 The NMRs were housed in acrylic chambers maintained at 30 ± 0.5°C, each of which

643 was assigned a different use. In the nest chamber, NMRs shared heat and became

644 warm by huddling together.

645

Figure S2. Characterization of naked mole-rat (NMR; *Heterocephalus glaber*) brown adipose tissue (BAT)

(a) Schematic diagram showing the location of BAT in NMRs. **(b)** Hematoxylin–eosin (HE)-stained images of ventral light BAT (vlBAT). Scale bar = 100 μm for the HE-stained image, 25 μm for inset. **(c)** Lipid droplet size in NMR-dBAT and mouse-interscapular BAT (Ms iBAT). A total of 50 droplets were measured from three different fields of view per tissue type. The data were analyzed using an unpaired *t*-test. **(d)** Percentage of total BAT (light BAT [lBAT], dark BAT [dBAT], and vlBAT) per gram body weight. The data are presented as means ± SD (n = 5 animals). **(e)** Relative expression levels of brown or beige adipocyte marker genes reported in mouse and human in NMR adipose tissues. Expression levels were quantified by quantitative polymerase chain reaction (qPCR) using the primers listed in Table S1 and were normalized to beta-actin (*ACTB*) (n = 3 animals). ingWAT, inguinal white adipose tissue (WAT) (control); gWAT, gonadal WAT; rpWAT, retroperitoneal WAT. The data are presented as means ± SEM and were analyzed using one-way analysis of variance followed by Dunnett's multiple comparison test with a single pooled variance (* $p < 0.05$ significantly different from ingWAT). **(f)**

662 Gene Ontology enrichment analysis of the top 200 upregulated genes in the dBAT

663 transcriptome using Metascape.

664

665

666 **Figure S3. Uncoupling protein 1 (UCP1) expression in the naked mole-rat (NMR;**

667 ***Heterocephalus glaber*)**

668 **(a)** UCP1 expression was evaluated by western blotting in NMR-dBAT, NMR-lBAT, and

669 NMR-iWAT. **(b)** Ponceau-S staining was performed for the membrane used **(a)** after the

670 UCP1 detection.

671

672

673

674

675

676

677

678

679

680

681

Figure S4. Correlation between brown adipose tissue (BAT) temperatures monitored with a thermo-probe and cervix surface temperatures monitored with a thermal camera

(a, b) Temperatures of the thermostable objects (**a;** 34.6°C–34.9°C, **b;** 31°C, measured by a mercury thermometer) were monitored by the thermal camera at various distances (four technical replicates at each point). Data are presented as means ± SEM * $p < 0.05$ (analyzed using one-way analysis of variance followed by Dunnett's multiple comparison test with a single pooled variance (* $p < 0.05$ significantly different from 10 cm). In this experiment, we used the thermopack (Sugiyama-Gen, Japan) as a thermostable object. **(c)** BAT temperatures and the maximum cervix surface temperatures of anesthetized subordinates were simultaneously recorded by a thermo-probe and thermal camera, respectively, every 1 min during the increase in body temperature, following the injection of 1 mg/kg noradrenaline ($n = 3$ animals).

Figure S5. Relationships between the body temperature and body weight, age, and sex of socially isolated subordinate naked mole-rats (NMRs; *Heterocephalus glaber*)

Maximum cervix surface temperatures of socially isolated subordinate NMRs monitored by thermal camera according to their (a) body weight, **(b)** age, and **(c)** sex. Data are presented as means ± SD. NS indicates nonsignificance (unpaired *t*-test).

705 **Video S1. Uptake of 2-deoxy-2-[18F]fluoro-D-glucose ([^{18}F]FDG) in the brown**

706 **adipose tissue (BAT) of naked mole-rats (NMRs; *Heterocephalus glaber*)**

707 The NMRs were administered 1 mg/kg noradrenaline, after which 11 MBq [^{18}F]FDG was

708 injected into the abdominal cavity. Positron emission tomography/computed

709 tomography (PET-CT) images were then acquired 1 h after [^{18}F]FDG administration.

710 The oblong signal is a microchip for individual identification.

711

712

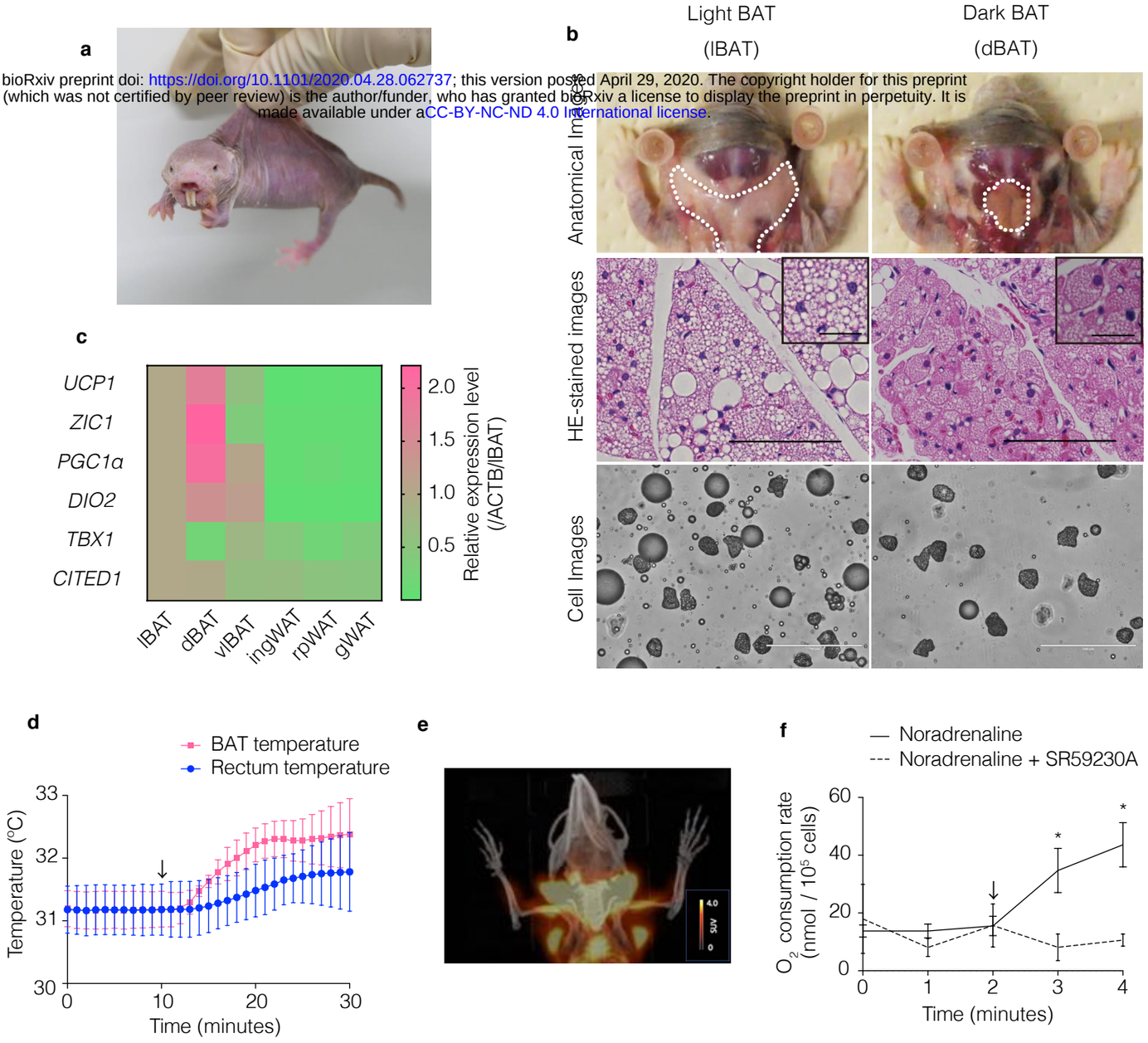

Figure 1. Poikilothermic naked mole-rats (NMRs; *Heterocephalus glaber*) possess thermogenic brown adipose tissue (BAT).

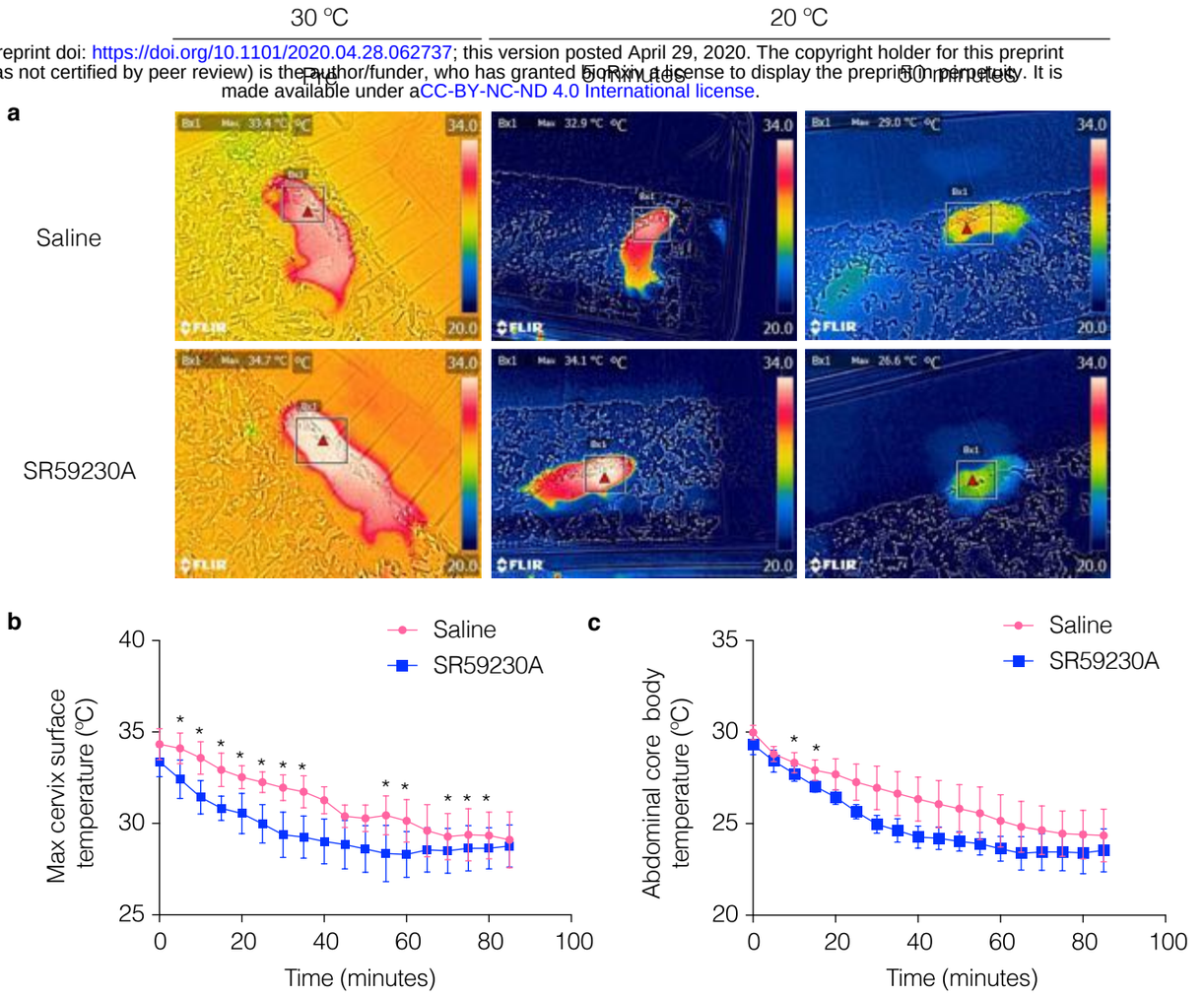

Figure 2. Brown adipose tissue (BAT) thermogenesis in naked mole-rat (NMR; *Heterocephalus glaber*) subordinates after cold exposure.

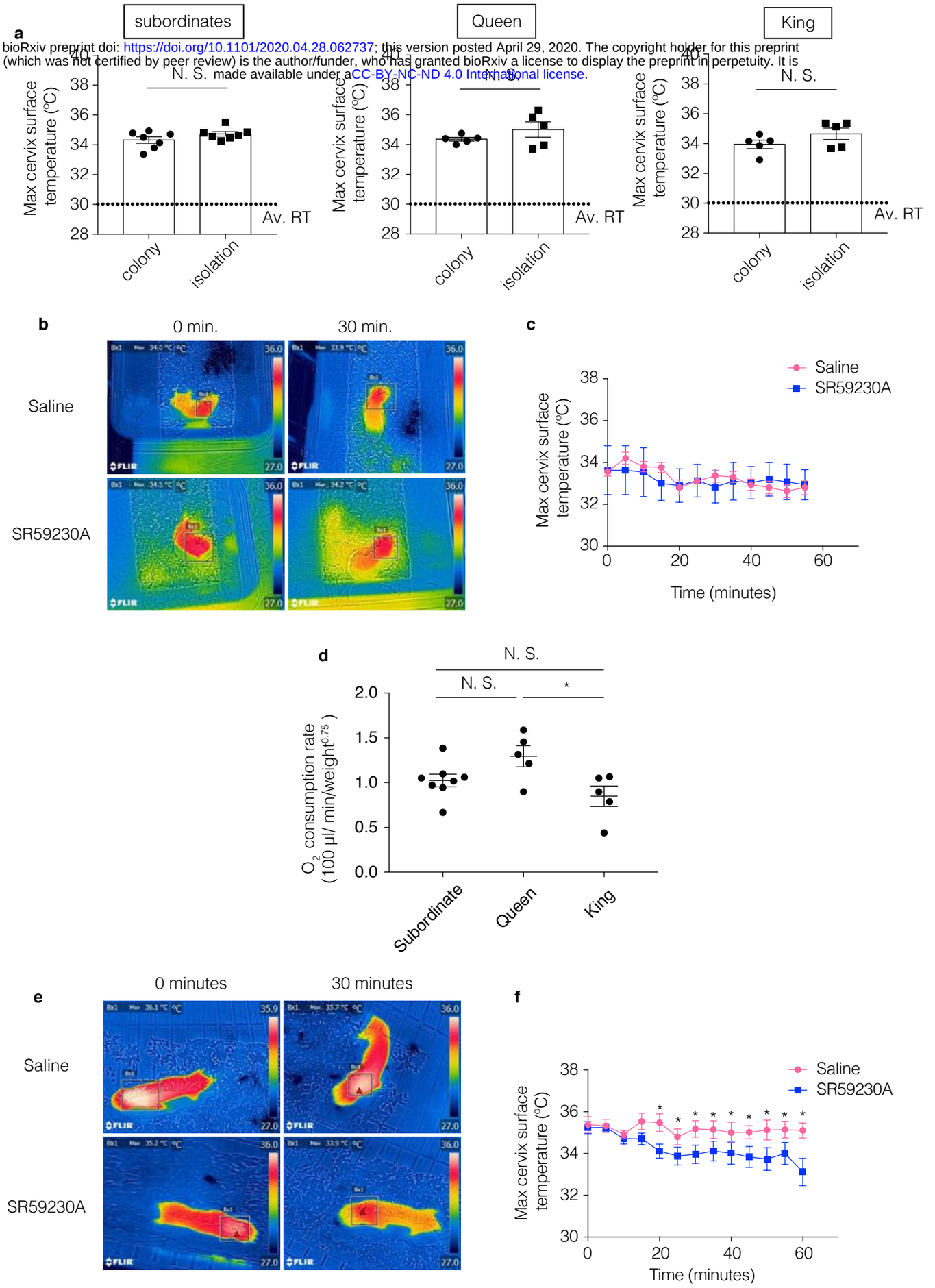

Figure 3. Isolated naked mole-rat (NMR; *Heterocephalus glaber*) queen exhibits BAT thermogenesis.

Figure S1. Images of the acrylic chambers connected by acrylic tunnels that were used to house the naked mole-rats (NMRs; *Heterocephalus glaber*) in the laboratory.

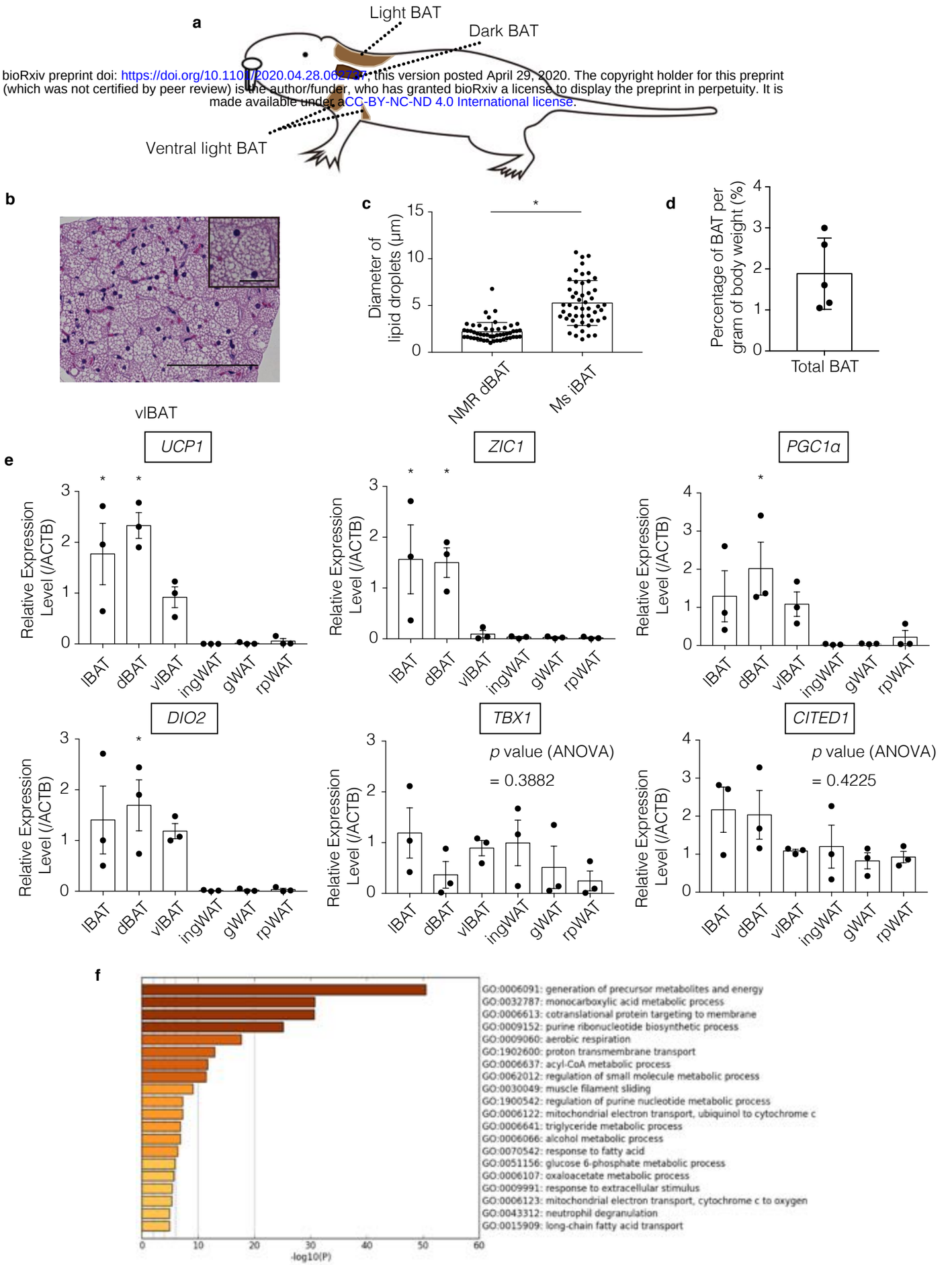

Figure S2. Characterisation of naked mole-rat (NMR; *Heterocephalus glaber*) brown adipose tissue (BAT).

Figure S3. UCP1 expression in the naked mole-rat (NMR; *Heterocephalus glaber*) brown adipose tissue (BAT).

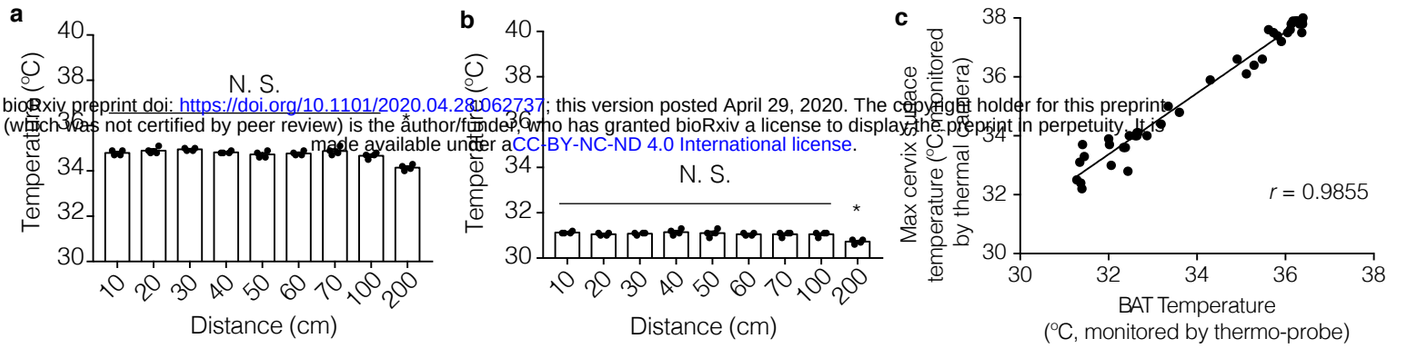

Figure S4. Correlation between brown adipose tissue (BAT) temperatures monitored with a thermo-probe and cervix surface temperatures monitored with a thermal camera.

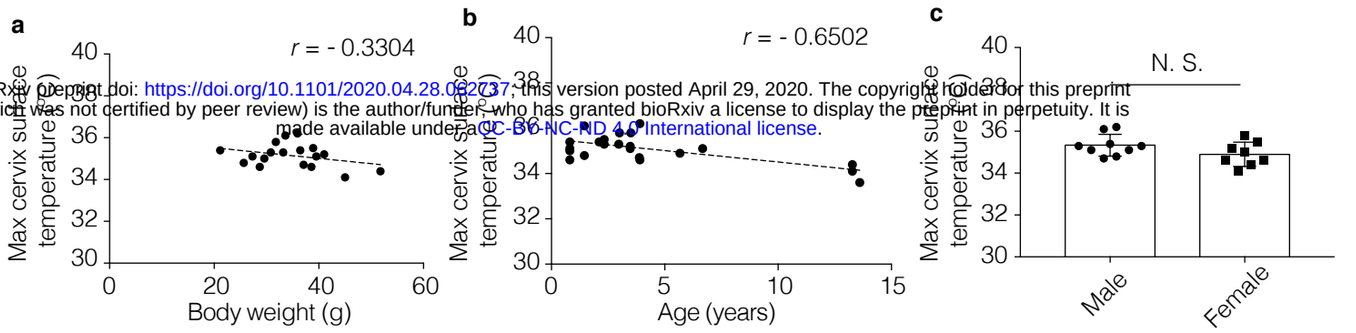

Figure S5. Relationships between the body temperature and body weight, age and sex of socially isolated subordinate naked mole-rats (NMRs; *Heterocephalus glaber*).

Table S1. Primer Sequences

NMR-UCP1-F	CCCATTCCAGTGATGTTGGTG
NMR-UCP1-R	TGCTCAAAGCACACAAACAT
NMR-ZIC1-F	AGCCCTTCAAGTGCGAGTTCGAG
NMR-ZIC1-R	CTTGCAGAGATAGGGCTTGTCAC
NMR-PGC1α-F	CACAGGATCAGAACAAACCC
NMR-PGC1α-R	CAGATACTTGAGAAGCTCCGA
NMR-DIO2-F	AGCTTTCTGCTCGATGCC
NMR-DIO2-R	TCCTGGACACCGTTTCCGCTA
NMR-TBX1-F	ACGGCCACATTATTCTCAACTCCA
NMR-TBX1-R	AAGCGCGTCTCCTCGAACACA
NMR-CITED1-F	CCGGCCCTTCGCTTTCACAC
NMR-CITED1-R	TCAGCTCAGTGGTGCCCCTT
NMR-ACTB-F	AGA CCT TCA ACA CCC CAG CCA TGT
NMR-ACTB-R	GGC CAG CCA GGT CCA GAC GCA G